

Istituto
Nazionale
Fisica
Nucleare

Sezione SANITÀ
Istituto Superiore di Sanità
Viale Regina Elena 299
I-00161 Roma, Italy

INFN-ISS 96/4
May 1996

Weak Decay Form Factors of Heavy Pseudoscalar Mesons within a Light-Front Constituent Quark Model

I.L. Grach^(a), I.M. Narodetskii^(a), S. Simula^(b)

^(a)Institute for Theoretical and Experimental Physics,
117259 Moscow, Russia

^(b)Istituto Nazionale di Fisica Nucleare, Sezione Sanità,
Viale Regina Elena 299, I-00161 Roma, Italy

Abstract

The transition form factors describing the semileptonic decays of heavy pseudoscalar mesons are investigated within a relativistic constituent quark model formulated on the light-front. For the first time, the form factors are calculated in the whole accessible kinematical region, adopting meson wave functions derived from various effective $q\bar{q}$ interactions able to describe the meson mass spectra. It is shown that the decay rates of the $B \rightarrow D\ell\nu_\ell$, $D \rightarrow K\ell\nu_\ell$ and $D \rightarrow \pi\ell\nu_\ell$ weak decays are mainly governed by the effects of the confinement scale, whereas the $B \rightarrow \pi\ell\nu_\ell$ decay rate is sensitive to the high-momentum components generated in the meson wave functions by the effective one-gluon-exchange interaction. Our results are consistent with available experimental data and predictions of lattice QCD calculations and QCD sum rules.

PACS numbers: 13.20.He; 13.20.Fc; 12.39.Ki; 12.15.Hh

Keywords: semileptonic decays; heavy mesons; relativistic quark model.

The investigation of semileptonic heavy-quark decays is an important test of our understanding of weak and strong interactions. As is well known, the semileptonic decay amplitude factorizes into the product of the leptonic and hadronic $V-A$ currents. The matrix elements of the latter contain relevant pieces of information about the strong forces which bind quarks and gluons into hadrons, whereas the leptonic part depends on the Cabibbo-Kobayashi-Maskawa (CKM) mixing parameters, $V_{Q_1 Q_2}$, which are fundamental quantities of the Standard Model. In order to calculate the decay rates and, hence, to extract the CKM parameters from the experiments, it is necessary to know the hadron form factors in the whole region of accessible values of the squared four-momentum transfer, $0 \leq q^2 \leq q_{max}^2$. It should be pointed out that till now the predictions obtained within various non-perturbative approaches, like, e.g., the QCD sum rule technique and the constituent quark (CQ) model, do not cover the full range of q^2 . In particular, as far as CQ models are concerned, the weak hadron form factors are usually calculated at a fixed value of q^2 (appropriate for the specific CQ model) and then extrapolated to the whole range of q^2 . As a matter of fact, in the original WSB approach [1] the form factors are calculated at $q^2 = 0$ and then extrapolated to $q^2 > 0$ using a monopole ansatz $1/(1 - q^2/M_{pole}^2)$, with M_{pole} being the mass of the lowest-lying vector meson in the given channel. Within the $ISGW$ model [2] the form factors are calculated at the point of zero recoil (i.e., $q^2 = q_{max}^2$) and then extrapolated to $q^2 = 0$ using an exponential-like ansatz. The CQ model of Ref. [3] uses the light-front (LF) formalism to compute the form factors for space-like values of q^2 ; then, the extrapolation to the time-like region is performed using a two-parameter formula, which reproduces the values of the form factors and their first two derivatives at $q^2 = 0$. Finally, in Ref. [4] the form factors have been calculated in the space-like region using a dispersion integral approach and, then, analytically continued in the time-like one.

In Ref. [5] the q^2 dependence of various heavy-to-heavy and heavy-to-light form factors among pseudoscalar mesons has been calculated in the whole accessible kinematical region. The calculations have been based on a LF CQ model, adopting a gaussian-like ansatz for the meson wave functions, and carried out in a reference frame where the momentum transfer is purely longitudinal, i.e. in a frame appropriate for time-like values of q^2 . It has been shown [5] that the time-like LF result, obtained using the matrix element of the "good" component of the weak vector current $J^+ = J^0 + J^3$, coincides with the contribution of the so-called spectator pole of the Feynman triangle diagram. The remaining part of the Feynman diagram, the so-called Z-graph, corresponds to the contribution of quark-pair creation from the vacuum. The Z-graph contribution is expected to be marginal for heavy-to-heavy decays (see [5]) and to become more important near the zero-recoil point for heavy-to-light decays (see [6]). In this letter we use the approach of Ref. [5], but, as far as the wave functions of the initial and final pseudoscalar mesons are concerned, we adopt the eigenfunctions of LF mass operators, constructed using various effective $q\bar{q}$ interactions able to reproduce the meson mass spectra. In this way a link between heavy-meson weak decay properties and the "spectroscopic" constituent quark model is explicitly constructed. It is shown that the decay rates for the $B \rightarrow D\ell\nu_\ell$, $D \rightarrow K\ell\nu_\ell$ and $D \rightarrow \pi\ell\nu_\ell$ decays are mainly governed by the effects of the confinement scale, whereas the $B \rightarrow \pi\ell\nu_\ell$ decay rate and, hence, the extraction of $|V_{ub}|$

are sensitive to the high-momentum components generated in the meson wave functions by the effective one-gluon-exchange (*OGE*) interaction. Our results obtained both for the form factors and the decay rates are compared with available experimental data and predictions of various non-perturbative approaches, like, e.g., lattice *QCD* simulations and *QCD* sum rules.

Here and below we denote by P_1 (P_2) and M_1 (M_2) the four-momenta and masses of the parent (daughter) mesons, respectively. The momenta and masses of the corresponding active quarks will be denoted as p_1 (p_2) and m_1 (m_2), whereas k (m) is the momentum (mass) of the light spectator (anti)quark. The four-momentum transfer is $q = P_1 - P_2$ and the fraction y is defined as $y = P_2^+/P_1^+$, where $P^+ \equiv P^0 + P^3$ with the 3-axis defining the spin quantization axis. In a frame where the three-momentum transfer is purely longitudinal (i.e., $\vec{q}_\perp = 0$), it can be easily verified that: $q^2 = (1 - y)(M_1^2 - M_2^2/y)$. Thus, one gets: $y_{1,2} = \zeta(\eta \pm \sqrt{\eta^2 - 1})$, where $\zeta = M_2/M_1$ and $\eta = U_1 \cdot U_2$, with U_1 and U_2 being the four-velocities of the parent and daughter mesons, respectively. The two signs for $y_{1,2}$ correspond to whether the three-momentum transfer is in the positive or negative direction of the 3-axis. At the point of zero recoil, $q^2 = q_{max}^2 = (M_1 - M_2)^2$, one has $y_1 = y_2 = \zeta$, while $y_1 = 1$ and $y_2 = \zeta^2$ at $q^2 = 0$.

The semileptonic decay of a pseudoscalar meson $Q_1\bar{q}$ into another pseudoscalar meson $Q_2\bar{q}$ is governed by the weak vector current only. The transition form factors $h_\pm(q^2)$ and $f_\pm(q^2)$ are defined as

$$\begin{aligned} \langle P_2 | \bar{Q}_2 \gamma_\mu Q_1 | P_1 \rangle &= \sqrt{M_1 M_2} \left[h_+(q^2) (U_1 + U_2)_\mu + h_-(q^2) (U_1 - U_2)_\mu \right] \\ &= f_+(q^2) (P_1 + P_2)_\mu + f_-(q^2) (P_1 - P_2)_\mu \end{aligned} \quad (1)$$

Neglecting lepton masses, the inclusive semileptonic decay rate Γ is given by

$$\Gamma = |V_{Q_1 Q_2}|^2 \frac{G_F^2 M_1^5}{12\pi^3} \zeta^4 \int_1^{\eta_{max}} d\eta (\eta^2 - 1)^{3/2} f_+^2(\eta) \quad (2)$$

where $\eta_{max} = (\zeta + 1/\zeta)/2$ and $V_{Q_1 Q_2}$ is the relevant *CKM* matrix element. The form factors $f_\pm(q^2)$ and $h_\pm(q^2)$ can be evaluated using only the "good" component of the current $J^+ = \bar{Q}_2 \gamma^+ Q_1$. The matrix elements of J^+ depend upon both q^2 and y , whereas the form factors f_\pm (h_\pm) are independent of y . In order to invert Eq. (1), two matrix elements $J^+(q^2, y) \equiv \langle P_2 | \bar{Q}_2 \gamma^+ Q_1 | P_1 \rangle$, corresponding to $y = y_1$ and $y = y_2$, should be calculated, obtaining: $J^+(q^2, y_i) = 2P_1^+ [f_+(q^2) (1 + y_i) + f_-(q^2) (1 - y_i)]$ with $i = 1, 2$. Putting $H(q^2, y_i) \equiv J^+(q^2, y_i)/2P_1^+$ one has

$$f_\pm(q^2) = \frac{(y_2 \mp 1)H(q^2, y_1) - (y_1 \mp 1)H(q^2, y_2)}{y_2 - y_1} \quad (3)$$

Following Ref. [5], the *LF* ground state of the parent meson $Q_1\bar{q}$ can be written as

$$|P_1 \rangle = \sum_{\lambda\bar{\lambda}} \int \frac{d\vec{k}_\perp}{\sqrt{2(2\pi)^3}} \frac{dx}{\sqrt{x(1-x)}} \sqrt{A_1(x, k_\perp^2)} R_{00}^{(1)}(x, \vec{k}_\perp; \lambda\bar{\lambda}) \frac{w_1(k^2)}{\sqrt{4\pi}} Q_1^\dagger \bar{q}^\dagger |0 \rangle \quad (4)$$

where $Q_1^\dagger \equiv Q_1^\dagger(\vec{p}_1, \lambda)$ and $\bar{q}^\dagger \equiv \bar{q}^\dagger(\vec{k}, \bar{\lambda})$ are the creation operators of the heavy active quark and the light spectator antiquark, with helicities λ and $\bar{\lambda}$, respectively. The LF momenta are taken as: $\vec{k} = (k^+, \vec{k}_\perp)$ and $\vec{p}_1 \equiv \vec{P}_1 - \vec{k} = (P_1^+ - k^+, -\vec{k}_\perp)$, where \vec{k}_\perp is the relative transverse momentum. The spectator and the active quarks carry the fractions x and $1-x$ of the plus component of the momentum of the meson, respectively. In Eq. (4) $R_{00}^{(1)}(x, \vec{k}_\perp; \lambda \bar{\lambda})$ is the momentum-dependent spin part of the meson wave function, arising from the Melosh rotations of the CQ spins (see [5]), and $A_1(x, k_\perp^2) \equiv M_{10}[1 - (m_1^2 - m^2)^2/M_{10}^4] / 4x(1-x)$, with $M_{10}^2 = (m_1^2 + k_\perp^2)/(1-x) + (m^2 + k_\perp^2)/x$ being the squared free mass. Finally, $k^2 \equiv k_\perp^2 + k_3^2$, where $k_3 \equiv (x - 1/2)M_{10} + (m_1^2 - m^2)/2M_{10}$. The state vector of the daughter meson has a form analogous to (4) with the obvious replacement $1 \leftrightarrow 2$. The states $|P_i\rangle$ ($i = 1, 2$) are normalized as: $\langle P'_i | P_i \rangle = (2\pi)^3 2P_i^+ \delta(P_i^+ - P'^i_+)$, so that the normalization condition for $w_i(k^2)$ is $\int_0^\infty dk^2 w_i^2(k^2) = 1$. Putting $x' \equiv x/y$ for the LF momentum fraction of the spectator quark in the final meson, the matrix elements $H(q^2, y)$ can be cast in the following form [5]

$$H(q^2, y) = \int_0^y dx \int d\vec{k}_\perp \sqrt{A_1(x, k_\perp^2) A_2(x', k_\perp^2)} \frac{w_1(k^2)w_2(k'^2)}{4\pi} \frac{[m(1-x) + xm_1] [m(1-x') + x'm_2] + k_\perp^2}{\sqrt{[m(1-x) + xm_1]^2 + k_\perp^2} \sqrt{[m(1-x') + x'm_2]^2 + k_\perp^2}} \quad (5)$$

The radial wave function $w_i(k^2)$ can be chosen to be the eigenfunction of an equal-time effective $Q\bar{q}$ Hamiltonian (see for more details [7]). For the latter we will consider two choices: the first one corresponds to the relativized Godfrey-Isgur (GI) Hamiltonian [8] and the second one is the non-relativistic (NR) model of Ref. [9]. We want to point out that both potential models nicely reproduce the mass spectra of light as well as heavy mesons. In particular, the interaction terms contain an effective OGE interaction, composed by a spin-dependent part, responsible for the hyperfine mass splitting in light mesons, and a spin-independent term, responsible for the hydrogen-like pattern of heavy-meson (bottomium) states. For comparison, we consider also a Gaussian-like ansatz, with the harmonic oscillator (HO) length taken from the updated version of the $ISGW$ model [10]. In what follows, the three choices will be referred to as the GI , NR and HO cases, respectively. The CQ momentum distribution corresponding to the wave functions $w^{(GI)}$, $w^{(NR)}$ and $w^{(HO)}$, obtained for the D -meson, is shown in Fig. 1. It can be seen that: i) $w^{(HO)}(k^2)$ is quite similar to the wave function obtained by retaining only the confining part of the GI interaction, i.e. it takes into account only the effects of the confinement scale; ii) both $w^{(GI)}$ and $w^{(NR)}$ exhibit high-momentum components generated by the effective OGE term; iii) the high-momentum tail is higher for the GI interaction. Similar results (cf. [7]) hold as well in case of the other mesons (π , K and B) considered in this letter.

The results obtained for the form factor $f_+(q^2)$ (Eqs. (3) and (5)) and the decay rate Γ (Eq. (2)) of the $B \rightarrow D\ell\nu_\ell$, $B \rightarrow \pi\ell\nu_\ell$, $D \rightarrow K\ell\nu_\ell$ and $D \rightarrow \pi\ell\nu_\ell$ decays, are reported in Tables 1-3 and Figs. 2-3, and compared with results from lattice QCD calculations, QCD sum rules and quark models. In our calculations the PDG [11] values of the meson masses have been adopted for all the three models of the meson wave function.

Decay $B \rightarrow D\ell\nu_\ell$. From Table 1 it can be seen that our results for $f_+^{B \rightarrow D}(q^2 = 0)$, $f_+^{B \rightarrow D}(q_{max}^2)$ and the decay rate $\Gamma(B \rightarrow D\ell\nu_\ell)$ depend only slightly upon the choice of the meson wave function, i.e. these quantities are mainly governed by the effects of the confinement scale. Our calculated rates are in agreement with existing CQ model predictions, which typically range from ~ 7 to $\sim 13 \text{ ps}^{-1}$. By combining the branching ratio $Br(B^0 \rightarrow D^- \ell^+ \nu_\ell) = (1.9 \pm 0.5)\%$ [11] with the world average of the B^0 lifetime, $\tau_{B^0} = 1.50 \pm 0.11 \text{ ps}$ [11], the measured rate is $\Gamma(B^0 \rightarrow D^- \ell^+ \nu_\ell) = (1.27 \pm 0.35) \cdot 10^{10} \text{ s}^{-1}$. From our predicted rates (see Table 1), one gets: $|V_{bc}| = 0.034 \pm 0.005$ (GI) and $|V_{bc}| = 0.036 \pm 0.005$ (NR and HO). These predictions, which are expected to be modified only slightly by radiative corrections (see [12]), are in agreement with the updated "experimental" determinations of $|V_{bc}|$ obtained from exclusive and inclusive semileptonic decays of the B -meson, viz. $|V_{bc}|_{excl} = 0.0373 \pm 0.0045_{exp} \pm 0.0065_{th}$ and $|V_{bc}|_{incl} = 0.0398 \pm 0.0008_{exp} \pm 0.0040_{th}$ [13]. At the point of zero recoil the form factor $h_+(\eta = 1)$ results to be: 0.960 (GI), 0.971 (NR), 0.965 (HO), in nice agreement with the updated QCD sum rule estimate, $1 + \delta_{1/m^2} = 0.945 \pm 0.025$ [12]. Moreover, the values of the slope, $\hat{\rho}^2$, and the curvature, \hat{c} , of the form factor $h_+(\eta)$ at the point of zero recoil, i.e. $h_+(\eta) \approx h_+(1)\{1 - \hat{\rho}^2(\eta - 1) + \hat{c}(\eta - 1)^2\} + O[(\eta - 1)^3]$, are: $\hat{\rho}^2 = 0.96$ (GI), 1.22 (NR), 1.30 (HO) and $\hat{c} = 0.71$ (GI), 0.96 (NR), 1.20 (HO). The results corresponding to the GI wave function compare very favourably with the recent model-independent improved bounds obtained in [14]. The full q^2 dependence of the form factor $f_+^{B \rightarrow D}(q^2)$ is shown in Fig. 2(a). It can be seen that: i) in the whole range of q^2 the form factor $f_+^{B \rightarrow D}(q^2)$ is affected only slightly by the high-momentum tail of the B - and D -meson wave functions; ii) the monopole approximation, with $M_{pole} = 6.25 \text{ GeV}$ [1], yields a slightly flatter q^2 dependence.

Decay $B \rightarrow \pi\ell\nu_\ell$. The q^2 dependence of the form factor $f_+^{B \rightarrow \pi}(q^2)$ is shown in Fig. 2(b). Near the zero-recoil point our result does not exhibit any pole dominance and deviates from recent results of lattice QCD simulations [15]. Such a discrepancy can be ascribed to the effects related to the admixture of the $|B^*\pi\rangle$ component in the B -meson wave function [6], which, in the LF language, corresponds to the contribution of the Z -graph (quark-pair creation diagram). We want to point out that the decay rate $\Gamma(B \rightarrow \pi\ell\nu_\ell)$ is not expected to be sharply affected by the Z -graph, because in Eq. (2) the contribution arising from the region near the zero-recoil point is kinematically suppressed. From Table 1 it can clearly be seen that the form factor $f_+^{B \rightarrow \pi}(q^2 = 0)$ and, hence, the decay rate $\Gamma(B \rightarrow \pi\ell\nu_\ell)$ are sensitive to the high-momentum components generated in the meson wave functions by the effective OGE interaction, particularly in case of the GI model. This feature is related to the huge value of the maximum recoil achieved in the $B \rightarrow \pi\ell\nu_\ell$ transition. Moreover, our LF results are in overall agreement with the ones obtained from recent lattice QCD simulations [15, 16], and only slightly lower than the results of the analysis performed in Ref. [17] using the LF QCD sum rule (see Tables 2-3). Recently, the $CLEO$ collaboration [20] has reported the first signal for exclusive semileptonic decays of the B meson into charmless final states, in particular for the decay channel $B \rightarrow \pi\ell\nu_\ell$. Adopting the models of Refs. [1] and [2] to reconstruct the efficiencies, the "model-dependent" branching ratios are: $Br(B \rightarrow \pi\ell\nu_\ell) = (1.63 \pm 0.57) \cdot 10^{-4}$ and $(1.34 \pm 0.45) \cdot 10^{-4}$, respectively.

Combining the average of these results with the world average value of the B^0 lifetime, one gets: $\Gamma(B^0 \rightarrow \pi^- \ell^+ \nu_\ell) = (0.99 \pm 0.25) \cdot 10^{-4} \text{ ps}^{-1}$. From our predicted rates (see Table 1) one has: $|V_{bu}| = 0.0025 \pm 0.0003$ (*GI*), 0.0030 ± 0.0004 (*NR*) and 0.0032 ± 0.0004 (*HO*). This means that the extraction of $|V_{ub}|$ is sensitive to the effects due to the high-momentum tail of the meson wave functions. We stress that this conclusion is not expected to be sharply modified by the effects related to the quark-pair creation from the vacuum. Using the results previously obtained for $|V_{bc}|$, one has: $|V_{bu}/V_{cb}| = 0.074 \pm 0.014$ (*GI*), 0.083 ± 0.016 (*NR*) and 0.088 ± 0.016 (*HO*). These results are in accord with the value of $|V_{bu}/V_{cb}|$ derived from measurements of the end-point region of the lepton spectrum in inclusive semileptonic decays [21, 22], viz. $|V_{bu}/V_{cb}|_{incl} = 0.08 \pm 0.01_{exp} \pm 0.02_{th}$.

Decay $D \rightarrow K \ell \nu_\ell$. The q^2 behaviour of the form factor $f_+^{D \rightarrow K}(q^2)$ is shown in Fig. 3(a). It can be seen that our form factor is mainly governed by the effects of the confinement scale and it is consistent both with the assumption of pole dominance and with the results of the lattice QCD calculations of Refs. [15, 23]. Moreover, our results for $f_+^{D \rightarrow K}(0)$ and $f_+^{D \rightarrow K}(q_{max}^2)$ (see Table 1) compare favourably with the recent experimental results [24] $f_+^{D \rightarrow K}(0) = 0.77 \pm 0.01 \pm 0.04$ and $f_+^{D \rightarrow K}(q_{max}^2) = 1.42 \pm 0.25$, obtained from the measured lepton spectrum assuming pole dominance. By combining the experimental data on the branching ratio, $Br(D^0 \rightarrow K^- e^+ \nu_e) = 3.68 \pm 0.21\%$ [11], with the accurate value of the D^0 lifetime, $\tau(D^0) = 0.415 \pm 0.004 \text{ ps}$ [11], one has: $\Gamma(D^0 \rightarrow K^- e^+ \nu_e) = 0.089 \pm 0.005 \text{ ps}^{-1}$. From our predicted rates (see Table 1) one obtains: $|V_{cs}| = 0.88 \pm 0.03$ (*GI*), 0.90 ± 0.03 (*NR*) and 0.89 ± 0.03 (*HO*). The constraint of unitarity of the CKM matrix with three generations of leptons yields a ($\sim 10\%$) higher value, viz. $|V_{cs}| = 0.974$ [11].

Decay $D \rightarrow \pi \ell \nu_\ell$. This is the only heavy-to-light decay where an extensive comparison with experiment is possible. Our results for the form factor $f_+^{D \rightarrow \pi}(q^2)$ are shown in Fig. 3(b). It can be seen that its behaviour at low q^2 agrees with the prediction of the LF QCD sum rule of Ref. [17], whereas near $q^2 = q_{max}^2$ it deviates from the pole approximation. The same discussion, already done about the relevance of the Z-graph in the $B \rightarrow \pi$ decay, applies as well to the $D \rightarrow \pi$ transition. From Tables 2-3 it can be seen that our values for $f_+^{D \rightarrow \pi}(q^2 = 0)$ and $\Gamma(D \rightarrow \pi \ell \nu_\ell)$ are in nice agreement both with the experimental data [11] and the results obtained within various non-perturbative approaches. Assuming $|V_{cd}| = 0.221 \pm 0.003$ [11] from the unitarity of the CKM matrix, our predictions for the semileptonic decay rate are: $\Gamma(D^0 \rightarrow \pi^- e^+ \nu_e) = 8.2 \pm 0.2$ (*GI*), 7.6 ± 0.2 (*NR*) and 7.8 ± 0.2 (*HO*), in units 10^{-3} ps^{-1} . These results compares favourably with the experimental value $(9.4^{+5.5}_{-2.9}) \cdot 10^{-3} \text{ ps}^{-1}$ [11] and the recent LF QCD sum rule prediction $(7.6 \pm 0.2) \cdot 10^{-3} \text{ ps}^{-1}$ [17]. The ratio of the branching fraction of the Cabibbo suppressed decay $D \rightarrow \pi \ell \nu_\ell$ to that of the Cabibbo favoured decay $D \rightarrow K \ell \nu_\ell$ has been recently determined by the CLEO collaboration by measuring both charged [25] and neutral [26] D -meson decays. Assuming the pole dominance for the form factors, the following values have been obtained: $|f_+^{D \rightarrow \pi}(0)/f_+^{D \rightarrow K}(0)| = 1.29 \pm 0.21 \pm 0.11$ [25] and $1.01 \pm 0.20 \pm 0.07$ [26]. With respect to the average of these values we predict a slightly lower ratio, viz. $|f_+^{D \rightarrow \pi}(0)/f_+^{D \rightarrow K}(0)| = 0.91$ (*GI*), 0.88 (*NR*) and 0.87 (*HO*). The value obtained in Ref. [10] is 0.71 and other theoretical predictions typically range from 0.7 to 1.4.

In conclusion, adopting a light-front constituent quark model we have investigated the transition form factors, which govern the heavy-to-heavy and heavy-to-light semileptonic weak decays between pseudoscalar mesons. For the first time, the form factors have been calculated in the whole kinematical region accessible in semileptonic decays, adopting meson wave functions derived from various effective $q\bar{q}$ interactions able to describe the meson mass spectra. It has been shown that the decay rates for the $B \rightarrow D\ell\nu_\ell$, $D \rightarrow K\ell\nu_\ell$ and $D \rightarrow \pi\ell\nu_\ell$ weak decays are mainly governed by the effects of the confinement scale, whereas the $B \rightarrow \pi\ell\nu_\ell$ decay rate and, hence, the extraction of $|V_{ub}|$ are sensitive to the high-momentum components generated in the meson wave functions by the effective one-gluon-exchange interaction. Our results both for the form factor and the decay rates are consistent with available experimental data and predictions of lattice QCD calculations and QCD sum rules. We want to stress that an estimate of the contribution of quark-pair creation from the vacuum is mandatory, particularly in case of the $B \rightarrow \pi\ell\nu_\ell$ and $D \rightarrow \pi\ell\nu_\ell$ transitions.

We are very grateful to K.A. Ter-Martirosyan for valuable discussions. Two of us (I.L.G. and I.M.N.) acknowledge the financial support of the INTAS grant No 93-0079. This work was done in part under the RFFR grant, Ref. No. 95-02-04808a.

References

- [1] M. Wirbel, B. Stech and M. Bauer: Z. Phys. **C29** (1985) 637.
- [2] N. Isgur, D. Scora, B. Grinstein and M.B. Wise: Phys. Rev. **D39** (1989) 799.
- [3] W. Jaus: Phys. Rev. **D41** (1990) 3394; *ib.* **D53** (1996) 1349.
- [4] D. Melikhov: Phys. Rev. **D53** (1996) 2460.
- [5] N.B. Demchuk, I.L. Grach, I.M. Narodetskii and S. Simula: preprint INFN-ISS 95/18 (hep-ph 9601369), to appear in Sov. J. of Nucl. Phys. (1996).
- [6] N. Isgur and M.B. Wise: Phys. Rev. **D41** (1990) 151.
- [7] F. Cardarelli *et al.*: Phys. Lett. **B332** (1994) 1; *ib.* **B349** (1995) 393; *ib.* **B359** (1995) 1; Few-Body Syst. Suppl. **9** (1995) 267; and to appear in Phys. Rev. **D53** (1996).
- [8] S. Godfrey and N. Isgur Phys. Rev. **D32** (1985) 185.
- [9] I.M. Narodetskii, R. Ceuleener and C. Semay: J. Phys. **G18** (1992) 1901.
- [10] D. Scora and N. Isgur: Phys. Rev. **D52** (1995) 2783.
- [11] Review of Particle Properties, L. Montanet *et al.*: Phys. Rev. **D50** (1994) 1173.

- [12] M. Neubert: Phys. Lett. **B338** (1994) 84.
- [13] T. Skwarnicki, preprint HEPSY-95-307, to appear in the Proc. of the 17th Int. Conf. on *Lepton-Photon Interactions*, Beijing, China, August 1995.
- [14] I. Caprini and M. Neubert: preprint CERN-TH/95-255, 1995.
- [15] C.R. Allton *et al.* (APE coll.): Phys. Lett. **B345** (1995) 513.
- [16] D.R. Burford *et al.* (UKQCD coll.): Nucl. Phys. **B447** (1995) 425.
- [17] A. Khodjamirian and R. Rückl: Nucl. Instr. and Meth. **A368** (1995) 28.
- [18] P. Ball: Phys. Rev. **D45** (1991) 3190.
- [19] C.A. Domingues and N. Paver: Z. Phys. **C41** (1988) 217; Phys. Lett. **B207** (1988) 499; **B211** (1988) 500(E).
- [20] R. Ammar *et al.* (CLEO coll.), contr. no. 0165 to the *EPS Conference*, Brussels, 1995.
- [21] H. Albrecht *et al.* (ARGUS coll.): Phys. Lett. **B255** (1991) 297.
- [22] J. Barlett *et al.* (CLEO coll.): Phys. Rev. Lett. **71** (1993) 4111.
- [23] C.W. Bernard *et al.*: Phys. Rev. **D43** (1991) 2140.
- [24] P.L. Fabretti *et al.* (E687 coll.): Phys. Lett. **364** (1995) 127.
- [25] M.S. Alam *et al.* (CLEO coll.): Phys. Rev. Lett. **71** (1993) 1311.
- [26] F. Butler *et al.* (CLEO coll.): Phys. Rev. **D52** (1995) 2656.

Table Captions

Table 1. The form factor $f_+(q^2)$ (Eqs. (3) and (5)) for various semileptonic decays, evaluated at $q^2 = 0$ and $q^2 = q_{\max}^2$ using the *GI*, *NR* and *HO* wave functions (see text), and the corresponding decay rate Γ (Eq. (2)), calculated in units ps^{-1} assuming $|V_{Q_1 Q_2}| = 1$.

Table 2. The form factor $f_+(q^2)$ of the $B \rightarrow \pi \ell \nu_\ell$ and $D \rightarrow \pi \ell \nu_\ell$ transitions evaluated at $q^2 = 0$ within different approaches. The label *Exp* means the experimental result (assuming pole dominance), while the labels *SR* and *LAT* correspond to *QCD* sum rule and lattice *QCD* calculations, respectively.

Table 3. The same as in Table 2, but for the decay rate Γ of the $B \rightarrow \pi \ell \nu_\ell$ and $D \rightarrow \pi \ell \nu_\ell$ transitions, calculated in units $10^{13}s^{-1}$ and $10^{11}s^{-1}$, respectively, assuming $|V_{Q_1 Q_2}| = 1$. The experimental result quoted for the $D \rightarrow \pi \ell \nu_\ell$ transition has been taken from [11] assuming $|V_{cd}| = 0.221$. The results from the lattice *QCD* simulations of Refs. [15, 16] are obtained assuming pole dominance.

Figure Captions

Fig. 1. The *CQ* momentum distribution $|w(k^2)|^2$ versus the internal momentum k in the *D*-meson. The solid, dashed and dotted lines correspond to the *GI*, *NR* and *HO* cases, respectively (see text). The dot-dashed line is the result obtained using the eigenfunction of the Hamiltonian of Ref. [8] in which only the confining part of the interaction term is retained.

Fig. 2. The form factor $f_+(q^2)$ of the $B \rightarrow D \ell \nu_\ell$ (a) and $B \rightarrow \pi \ell \nu_\ell$ (b) transitions. The solid, dashed and dotted lines correspond to the results of our *LF* calculations (Eq. (5)), obtained using the *GI*, *NR* and *HO* wave functions, respectively. The dot-dashed lines are the monopole approximation $f_+(q^2) = f_+(0)/(1 - q^2/M_{pole}^2)$ with $M_{pole} = 6.25 \text{ GeV}$ (a) and 5.33 GeV (b). In (b) the open dots and squares are the *QCD* sum rule predictions of Refs. [17] and [18], respectively, whereas the full dots are the lattice *QCD* results from Ref. [15].

Fig. 3. The same as in Fig. 2, but for the $D \rightarrow K \ell \nu_\ell$ (a) and $D \rightarrow \pi \ell \nu_\ell$ (b) transitions. The dot-dashed lines are the monopole approximation with $M_{pole} = 2.11 \text{ GeV}$ (a) and 2.01 GeV (b). The full triangles are the predictions of the lattice *QCD* simulations of Ref. [23].

Table 1

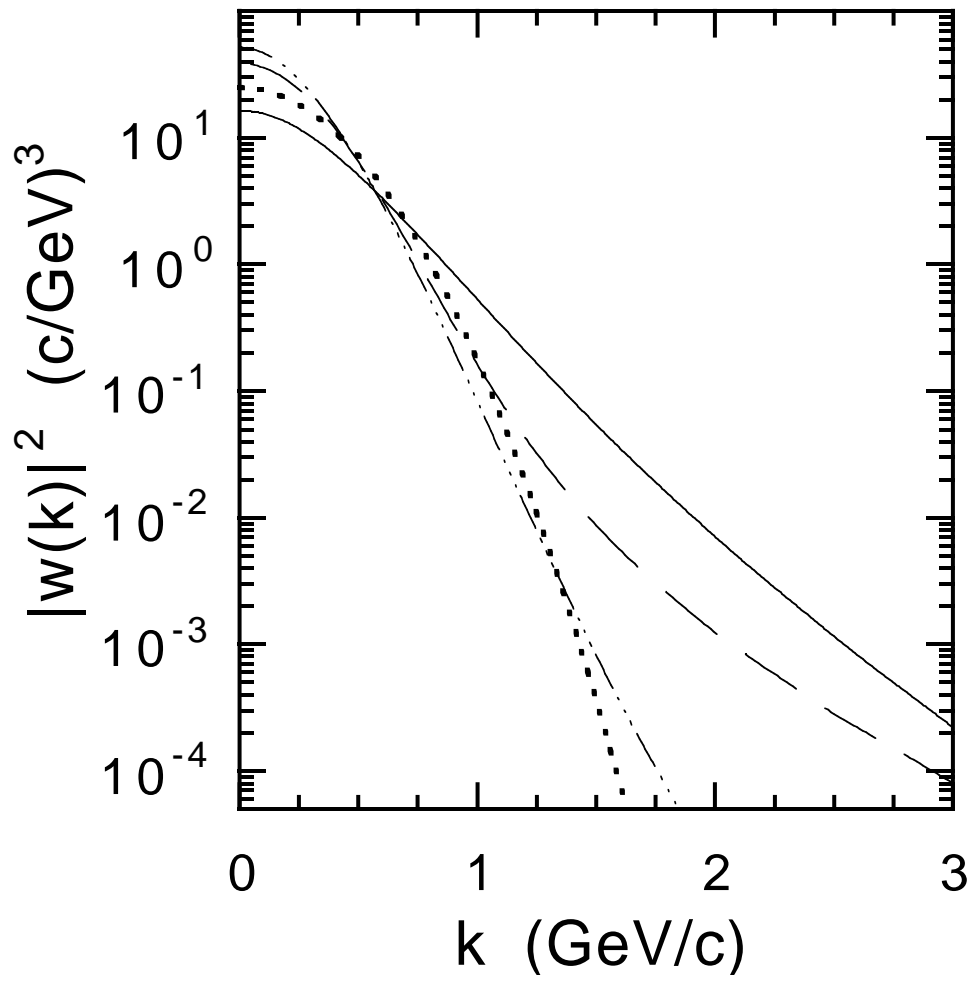
weak transition	wave function	$f_+(0)$	$f_+(q_{\max}^2)$	Γ
$B \rightarrow D$	GI	0.765	1.294	11.13
	NR	0.692	1.322	9.835
	HO	0.684	1.365	9.780
$B \rightarrow \pi$	GI	0.464	1.803	15.21
	NR	0.361	1.524	11.12
	HO	0.293	1.658	9.624
$D \rightarrow K$	GI	0.835	1.379	0.114
	NR	0.787	1.598	0.111
	HO	0.780	1.560	0.112
$D \rightarrow \pi$	GI	0.762	1.281	0.167
	NR	0.694	1.216	0.156
	HO	0.681	1.289	0.160

Table 2

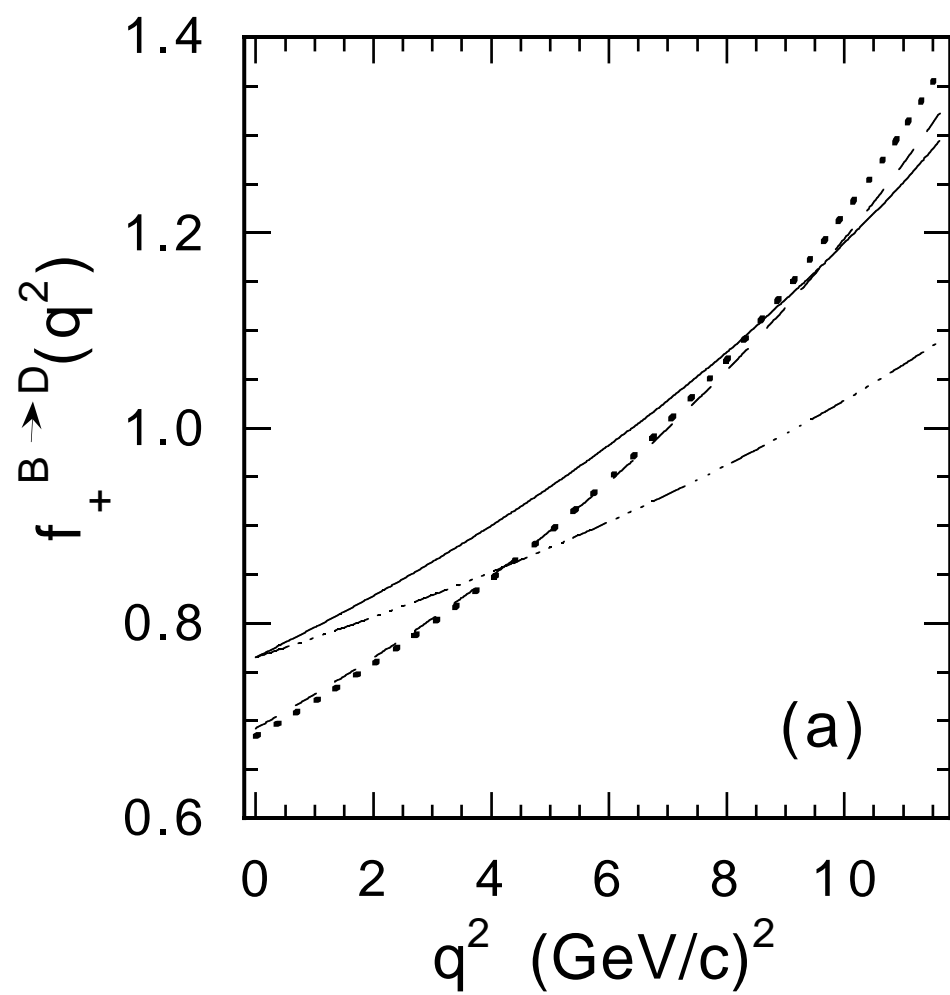
	$f_+^{B \rightarrow \pi}(0)$	$f_+^{D \rightarrow \pi}(0)$
GI	0.464	0.762
NR	0.361	0.694
HO	0.293	0.684
SR [17]	0.29 ± 0.01	0.66 ± 0.03
SR [18]	0.26 ± 0.02	0.5 ± 0.1
SR [19]	0.4 ± 0.1	0.75 ± 0.05
WSB [1]	0.33	0.69
ISGW [2]	0.09	0.51
LAT [15]	0.35 ± 0.08	0.80 ± 0.08
LAT [16]	0.43 ± 0.02	
Exp [11]		$0.75^{+0.23}_{-0.15} \pm 0.06$

Table 3

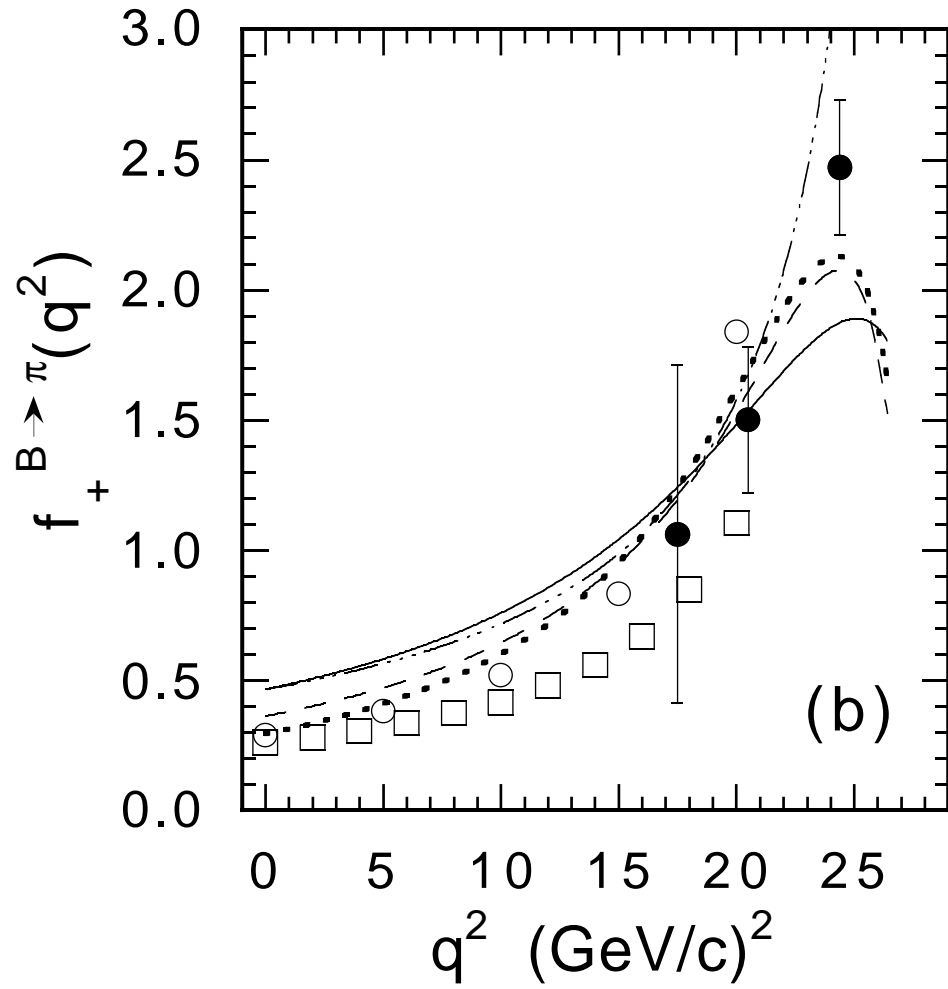
	$\Gamma(B^0 \rightarrow \pi^+ e^- \bar{\nu})$	$\Gamma(D^0 \rightarrow \pi^- e^+ \nu)$
GI	1.521	1.67
NR	1.112	1.56
HO	0.962	1.60
SR [17]	0.81	1.56
SR [18]	0.51 ± 0.11	0.80 ± 0.17
SR [19]	1.45 ± 0.59	$1.66^{+0.23}_{-0.21}$
WSB [1]	0.74	1.41
ISGW [2]	0.21	0.77
LAT [15]	0.8 ± 0.4	$1.8^{+0.6}_{-0.4}$
LAT [16]	1.02 ± 0.36	
Exp [11]		$1.9^{+1.1}_{-0.6}$



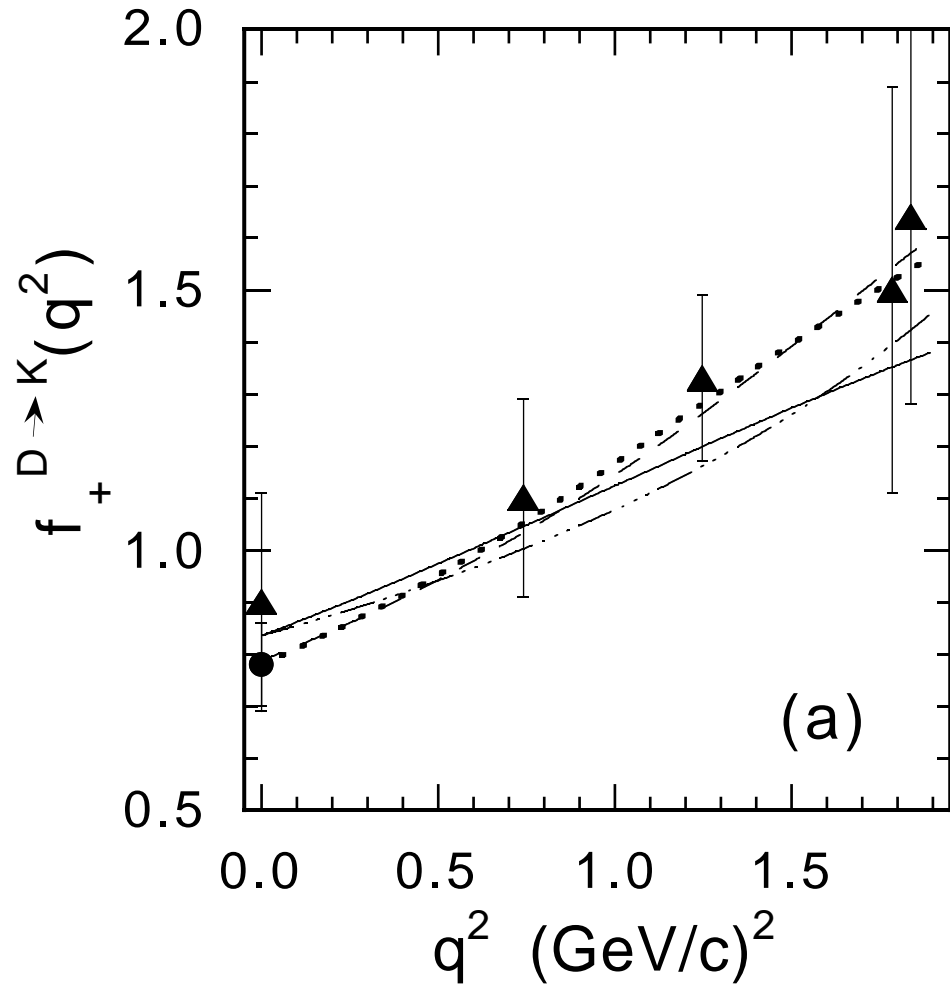
I.L. Grach, I.M. Narodetskii and S. Simula: fig. 1



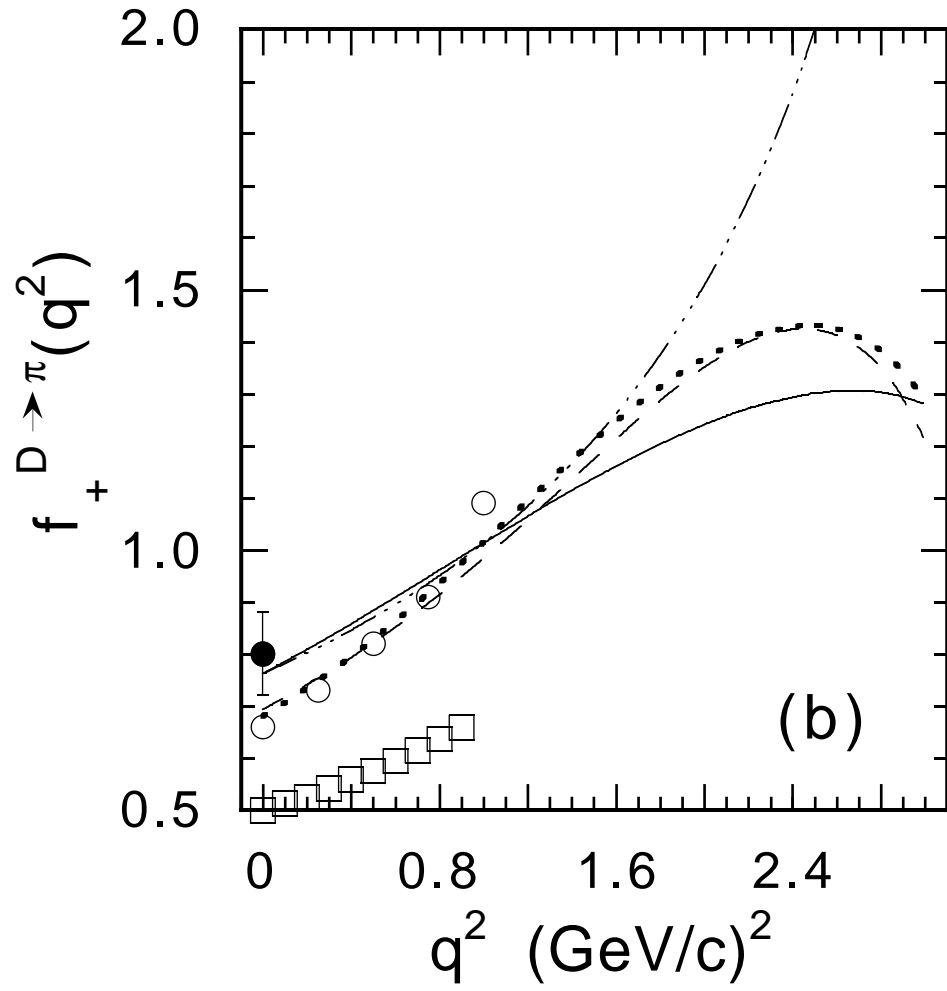
I.L. Grach, I.M. Narodetskii and S. Simula: fig. 2a



I.L. Grach, I.M. Narodetskii and S. Simula: fig. 2b



I.L. Grach, I.M. Narodetskii and S. Simula: fig. 3a



I.L. Grach, I.M. Narodetskii and S. Simula: fig. 3b